

# Size Selected Gold Cluster Supported Alumina as Catalyst in Reduction of 4-Nitrophenol to 4-Aminophenol

Mostafa Farrag<sup>1,\*</sup> and Samia Ibrahim<sup>2</sup>

<sup>1</sup>Chemistry Department, Faculty of Science, Assiut University, 71516 Assiut, Egypt.

<sup>2</sup> Department of Chemistry, Faculty of Science, Assiut University, New Valley Branch, El-Kharja 72511, New Valley, Egypt.

Received: 26 Oct. 2016, Revised: 12 Dec. 2016, Accepted: 18 Dec. 2016.

Published online: 1 Jul. 2017.

**Abstract:** The catalytic activity of one-pot synthesis gold clusters protected by L-glutathione is studied. Different sizes gold clusters Au<sub>25</sub>(SG)<sub>18</sub> and in average 1.5 nm and 3 nm Au<sub>n</sub>(SG)<sub>m</sub> are deposited over aluminium dioxide (Al<sub>2</sub>O<sub>3</sub> Puralox SCCa-190HPV). The synthesized clusters on alumina (1% Au<sub>n</sub>(SG)<sub>m</sub>/Al<sub>2</sub>O<sub>3</sub>) were tested as new catalysts in reduction of 4-nitrophenol (4-NP) in presence of aqueous NaBH<sub>4</sub>. The results showed that the 1% Au<sub>25</sub>(SG)<sub>18</sub>/Al<sub>2</sub>O<sub>3</sub> catalyst exhibited the best catalytic performance in the reduction of 4-NP into 4-aminophenol (4-AP) and revealed 100% conversion following 2 min stirring at room temperature. The catalyst weight was used in this reaction 0.3 g/L. The particles sizes and optical properties of synthesized clusters were investigated by transmission electron microscopy and UV–vis spectroscopy, respectively. The catalytic reduction reaction of 4-NP were followed by UV–vis spectroscopy. N<sub>2</sub> sorptiometry were used for the characterization of surface morphology, specific surface area S<sub>BET</sub>, pore volume and average pore diameter for synthesized clusters on alumina. The extreme catalytic activity of the small gold clusters attribute to their electronic properties. The partial positive charges of the surface gold atoms in the Au<sub>25</sub>(SR)<sub>18</sub> clusters should facilitate the electron transfer from the negatively charged BH<sub>4</sub><sup>-</sup> to 4-NP.

**Keywords:** Size selected gold nanoclusters; 4-Nitrophenol reduction; Al<sub>2</sub>O<sub>3</sub> Puralox SCCa-190 HPV; L-Glutathione; In dark.

## 1 Introduction

Catalysis by gold nanoparticles has attracted many research interest in recent years [1-3] and a wide range of reaction processes have been found to be catalyze by monolayer protected gold nanoclusters (1–3 nm) [2–7]. The turnover frequency (TOF) of carbon dioxide oxidation over supported gold catalysts is dependent on the size of Au particles [8,9], especially when Au nanoparticles are supported on the ‘non-reducible’ oxides such as Al<sub>2</sub>O<sub>3</sub>, SiO<sub>2</sub> and MgO [10].

Many methods have been used for the synthesis of Au nanoparticles, such as co-precipitation [11], colloidal deposition [12], deposition–precipitation [9], chemical vapor deposition [13] and photochemical methods [14]. However, these methods produce a very broad size distribution of Au nanoparticles (2-10 nm). Recently a successful size selected gold [15-22] and silver [15,23] nanoclusters has been prepared (typically <2 nm diameter). These gold clusters protected by thiolate ligands (denoted as Au<sub>n</sub>(SR)<sub>m</sub>, where n and m denote the number of gold atoms and thiolate ligands, respectively) [15-23].

The wide applications of amine compounds in photographic developers, corrosion inhibitors, anticorrosion-lubricants, and hair-dyeing agents induce the researcher to prepare amines by different ways such as reduction the nitro compounds to amines [24-32]. A great numbers of studies have been achieved for the reduction of p-nitrophenol to p-aminophenol over the last past decades [25–27]. These studies are used different reducing agents such as NaBH<sub>4</sub> in the presence of palladium nanoparticles [28], gold nanoparticles [29], silver nanoparticles [30] and hydrogen gas in the presence of Ni-B alloy catalysts [31], and iron powder or stannous chloride under ultrasonic irradiation [32].

In general, supported Ag catalysts exhibit lower hydrogenation activities relative to gold catalysts, especially when the

\*Corresponding author e-mail: [mostafafarrag@aun.edu.eg](mailto:mostafafarrag@aun.edu.eg)

particles size was less than 10 nm [33-38]. Monodisperse Au nanocrystals with an average diameter 8.2 nm were synthesized by using nontoxic and renewable biochemical  $\beta$ -d-glucose as reducing and capping agents. The prepared catalyst shows effective catalytic activity in reduction of 4-nitrophenol in the presence of  $\text{NaBH}_4$  [39]. M. M. Mohamed et al. [40] synthesized silver nanoparticles (5 nm), which were assembled in self-organized polyhedral  $\text{TiO}_2$  (17 nm). This catalyst showed high photoreduction performance in conversion of p-nitrophenol to p-aminophenol using visible light source (98% conversion in 2 min) [40].

The ultrasmall  $\text{Au}_{25}(\text{SCH}_2\text{CH}_2\text{Ph})_{18}$  cluster catalyzed the hydrogenation of carbonyl bond in  $\alpha,\beta$ -unsaturated ketones or aldehydes with 100% chemoselectivity towards the formation of  $\alpha,\beta$ -unsaturated alcohols even at low temperatures (e.g.  $0^\circ\text{C}$ ) [2]. For the sake of comparison the catalytic activity of different sizes gold clusters ( $\text{Au}_{25}(\text{SCH}_2\text{CH}_2\text{Ph})_{18}$ ,  $\text{Au}_{38}(\text{SCH}_2\text{CH}_2\text{Ph})_{24}$  and  $\text{Au}_{144}(\text{SCH}_2\text{CH}_2\text{Ph})_{60}$ ) was studied in oxidation of styrene [7]. The catalytic activity of clusters catalyst decreased with increase the particles size in oxidation of styrene [7].

In this paper we synthesized three different sizes gold clusters protected by L-glutathione  $\text{Au}_{25}(\text{SG})_{18}$ , 1.5 and 3 nm nanoparticles by a one-pot synthesis method. These nanoparticles are isolated by methanol-induced precipitation method with a controlled amount of added methanol. For first time, these nanoclusters were supported over  $\text{Al}_2\text{O}_3$  by impregnation method to use it as heterogeneous catalysts in reduction of 4-nitrophenol (4-NP) to 4-aminophenol (4-AP) in presence of  $\text{NaBH}_4$ . The textural features of the gold cluster on  $\text{Al}_2\text{O}_3$  catalysts were investigated using nitrogen adsorption-desorption at  $-196^\circ\text{C}$ . Specific surface area  $S_{\text{BET}}$ , pore volume and average pore diameter of the new catalysts were calculated. UV-vis spectroscopy and transmission electron microscope (TEM) were used to investigate the optical properties and the particle sizes on the prepared nanoclusters, respectively. The progress of the reduction reactions and the recyclability of the size selected gold clusters ( $\text{Au}_{25}$ ) over  $\text{Al}_2\text{O}_3$  catalyst were followed by UV-vis spectroscopy

## 2 Experimental

### 2.1 Chemicals

Tetrachloroauric (III) acid ( $\text{HAuCl}_4 \cdot 3\text{H}_2\text{O}$ , >99.99% metals basis, Sigma-Aldrich), Sodium borohydride ( $\text{NaBH}_4$ ,  $\geq 96\%$ , Aldrich), L-glutathione ( $\gamma$ -L-Glutamyl-L-cysteinyl-glycine,  $\gamma$ -Glu-Cys-Gly, L-GSH) reduced (98%, Sigma-Aldrich), were used for synthesizing the ligand protected gold nanoparticles. Aluminium dioxide ( $\text{Al}_2\text{O}_3$  Puralox SCCa-190HPV) was supported from Sasol Germany GmbH Company. Methanol (HPLC grade, Aldrich) was used to separate the nanoclusters from the aqueous mother solution. All chemicals were used as received. All glassware was thoroughly cleaned with aqua regia ( $\text{HCl}:\text{HNO}_3 = 3:1$  v/v), rinsed with 2<sup>nd</sup> distilled water and ethanol, and then dried in an oven prior to use.

### 2.2. Preparation of size selected gold clusters (1-3)

For the synthesis the three sizes selected clusters protected by L-glutathione, a one-pot synthesis, methanol-induced precipitation approach was employed [41,15]. Briefly, Tetrachloroauric (III) acid (52.0 mg) was dissolved in 26 mL 2<sup>nd</sup> distilled water, the solution was cooled to around  $0^\circ\text{C}$  in an ice bath over a period of 30 min. Then, 162 mg glutathione was slowly added to the solution under slow magnetic stirring (60 rpm); the solution turned clear after continuous stirring for 1.5 h. 50 mg  $\text{NaBH}_4$  (dissolved in 6.5 mL ice-cold water) was rapidly added to the clear gold salt solution under vigorous stirring (1100 rpm). The solution immediately became dark, indicating the reduction of gold salt and formation of nanoparticles. The reaction was allowed to proceed for about 12 h, then 16 mL  $\text{CH}_3\text{OH}$  was slowly added under stirring, the precipitates (fraction 1) were collected by centrifugation (3800 rpm, 10 min) and washed with 1 mL  $\text{CH}_3\text{OH}/\text{H}_2\text{O}$  (1:1, v/v), repeatedly washed by methanol (1 mL x 3). The supernatant from the first precipitation contained the smaller nanoparticles; more  $\text{CH}_3\text{OH}$  (32 mL) was added, and the precipitates (fraction 2) were collected by centrifugation (3800 rpm, 20 min), washed with 1 mL  $\text{CH}_3\text{OH}/\text{H}_2\text{O}$  (2:1, v/v), repeatedly washed by methanol (1 mL x 3). The two fractions were dried under reduced pressure over 3 hours. The remaining supernatant (fraction 3) showed absorption peaks characteristic of  $\text{Au}_{25}$ . After concentrating the solution,  $\text{Au}_{25}(\text{SG})_{18}$  was isolated by adding  $\text{CH}_3\text{OH}$ , then washed with  $\text{CH}_3\text{OH}$  (1 mL x 3) and dried in a vacuum desiccator at 25 mmHg in air atmosphere.

### 2.3. Preparation of gold clusters over $\text{Al}_2\text{O}_3$ Puralox SCCa-190HPV

The 1% Gold-clusters/ $\text{Al}_2\text{O}_3$  catalysts were prepared by well known impregnation method. 1 g  $\text{Al}_2\text{O}_3$  powder was dispersed into a 40 ml aqueous solution contains 10 mg from the corresponding gold clusters ( $\text{Au}_{25}(\text{SG})_{18}$ , 1.5 nm  $\text{Au}_n(\text{SG})_m$  and 3 nm  $\text{Au}_n(\text{SG})_m$ ). The slurry was stirred one day at room temperature, the brown color of gold clusters solution becomes colorless, confirming all the clusters amount were supported over the  $\text{Al}_2\text{O}_3$  surface. The precipitate was collected by centrifugation (6000 rpm, 10 min) and washed with  $\text{H}_2\text{O}$ , and then the catalysts were dried at  $100^\circ\text{C}$  in air

atmosphere.

#### 2.4. Activity measurements by catalytic reduction of 4-NP

To investigate the catalytic activity of prepared catalysts, 50 ml of 4-NP solution (2 mM) was added to 15 mg catalyst (1%  $\text{Au}_n(\text{SG})_m/\text{Al}_2\text{O}_3$ ), then 2.5 ml of  $\text{NaBH}_4$  (2 M) was added under constant stirring. The yellow color of solution gradually transformed to colorless, indicating the reduction of 4-NP into 4-AP, during the hydrogenation process. Samples were directly withdrawn from the reaction medium after certain regular interval stirring time followed by measuring UV-vis spectra of these solutions to monitor the decrease in intensity of the absorption peak at 400 nm for 4-NP and  $\text{NaBH}_4$  mixture. The progress of the reaction and the activation parameters for the reduction reaction of 4-NP to the corresponding amine was determined. At the end of the reaction, the catalysts were separated from the suspension by centrifugation (6000 rpm), washed several times with water and dried for 2 hrs at 110 °C, and then reused to study the recyclability of the prepared catalysts. The product 4-aminophenol was also identified by capillary column gas chromatography.

#### 2.5. Instrumentation and Characterization

To obtain the UV-vis absorption spectra of the prepared gold nanoclusters (1–3), aqueous solutions of approximately 1–2 mg/mL were prepared. The characteristic absorption peaks of 4-nitrophenol and 4-aminophenol were investigated also by UV-vis spectroscopy. The spectra of all the solutions were recorded at ambient temperature from 200 to 900 nm with a double-beam spectrophotometer (Evolution 300). For TEM measurements, solutions with a concentration of 1–2 mg/mL were prepared by dissolving the cluster materials in 2<sup>nd</sup> distilled water. A droplet of these AuNCs solutions was casted onto carbon-coated copper grids. The solvent was then allowed to evaporate slowly. TEM images were obtained with a high resolution transmission electron microscope (HRTEM) TECNAI G<sup>2</sup> spirit TWIN at acceleration voltage of 120 kV, conducted by VELETA Camera. The images were then analyzed by using Image J software (version 1.44). Adsorption-desorption isotherms of nitrogen at –196 °C were obtained using a Quantachrome (Nova 3200 series) multi-gas adsorption apparatus. Prior to analysis, the samples were degassed at 100°C for 2 hrs. Specific surface areas were calculated from these isotherms by applying the BET (Brunauer–Emmett–Teller) equation.  $S_t$  Values were calculated using the  $V_{a-t}$  plots of de Bore. To investigate the products a capillary column gas chromatography (Trace GC Ultra, Thermo Scientific) was used.

### 3 Results and Discussion

A one-pot synthesis of multiple size gold nanoclusters was prepared by methanol-induced precipitation method. The samples were further purified by several cycles of re-solution in water and re-precipitation by adding methanol. The as-prepared clusters were then characterized by UV-vis spectroscopy and transmission electron microscopy (TEM). The catalytic activity of the prepared clusters on  $\text{Al}_2\text{O}_3$  was studied by reduction of 4-nitrophenol to 4-aminophenol in presence  $\text{NaBH}_4$ . The surface properties of prepared catalysts were investigated by  $\text{N}_2$  sorptiometry.

#### 3.1. Characterization of Prepared Gold Nanoclusters (AuNCs)

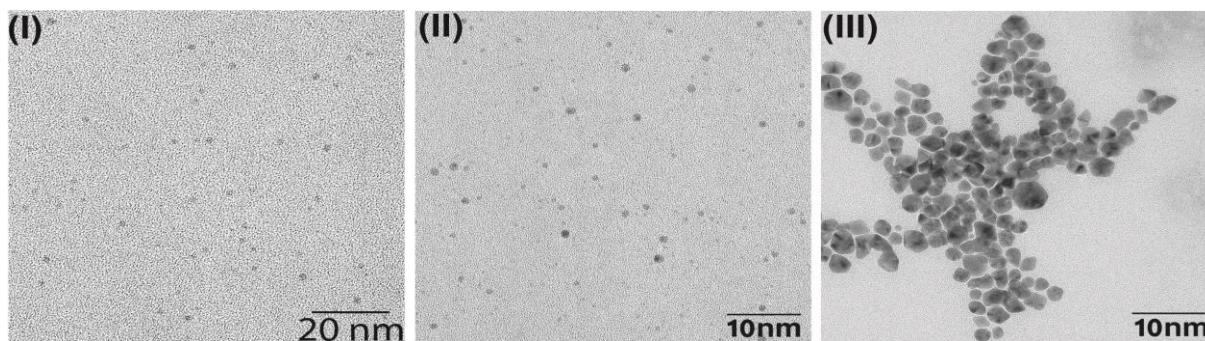


**Figure 1.** Transmission electron microscopy (TEM) images of (I)  $\text{Au}_{25}(\text{SG})_{18}$  clusters, the particles size of these clusters are around 1 nm with a very narrow size distribution, (II) fraction 2  $\text{Au}_n(\text{SG})_m$  nanoclusters with average diameter of 1.5 nm and (III) fraction 1  $\text{Au}_n(\text{SG})_m$  nanoclusters with average diameter of 3 nm.

Three major nanoparticles were produced in one pot and isolated by precipitation with different amounts of methanol. The larger nanoparticles (Fraction 1) are precipitated with only a small amount of added methanol, leaving smaller particles in the mother solution. By controlling the amount of methanol added, another two sizes were separated 1.5 nm (Fraction 2) and  $\text{Au}_{25}$  nanoparticles. Transmission electron microscopy (TEM) determined their average particle sizes, Fig.1 shows the

particles size of  $\text{Au}_{25}(\text{SG})_{18}$ , fraction 2, and fraction 1 nanoparticles, respectively. The average particle size of fraction 1 and fraction 2 are 3 nm and 1.5 nm, respectively. Fig. 1a shows the TEM image of the highly monodisperse clusters ( $\text{Au}_{25}(\text{SG})_{18}$ ), which evidenced by its absorption spectrum [15, 42]. The absorption spectrum of the third cut ( $\text{Au}_{25}(\text{SG})_{18}$ ) shows an interesting multi-band absorption spectrum with distinct peaks at around 400 nm, 450 nm, and 670 nm (Fig. 2c). These absorption bands indeed resemble the spectroscopic fingerprints of  $\text{Au}_{25}$  nanoclusters [15,21,42,43]. Fraction 1 (3 nm) shows a well-defined surface plasmon absorption band at 525 nm (Fig. 2a). The optical spectrum of fraction 2 (1.5 nm) shows an essentially decaying curve without the surface plasmon peak (Fig. 2b), which indicates that the particles of fraction 2 are too small to backup surface plasmon resonance.

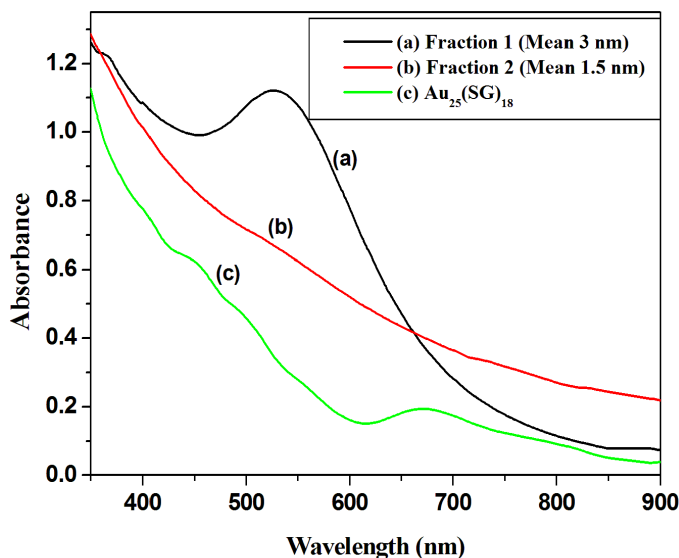


**Figure 2.** UV-vis absorption spectra of the three different size gold clusters, protected by L-glutathione ligand. (a) Fraction 1 of gold clusters (average size 3 nm) shows a well-defined surface plasmon absorption band at 534 nm. (b) Gold clusters of the second fraction (average size 1.5 nm) gives a featureless band without a distinct surface plasmon absorption peak. (c)  $\text{Au}_{25}(\text{SG})_{18}$  cluster shows a multi-band absorption spectrum with distinct peaks at around 400 nm, 450 nm and 670 nm, these absorption bands indeed resemble the spectroscopic fingerprints of  $\text{Au}_{25}$  nanoclusters.

### 3.2. Surface Texturing Analysis

The three size selected gold nanoclusters were supported over aluminium dioxide ( $\text{Al}_2\text{O}_3$  Puralox SCCa-190HPV) with doping percentage (1%) to prepare new three catalysts 1%  $\text{Au}_{25}(\text{SG})_{18}/\text{Al}_2\text{O}_3$ , 1% 1.5 nm  $\text{Au}_n(\text{SG})_m/\text{Al}_2\text{O}_3$  and 1% 3 nm  $\text{Au}_n(\text{SG})_m/\text{Al}_2\text{O}_3$ . The surface texture properties of these new catalysts were studied by measuring the adsorption–desorption isotherms.

The adsorption–desorption isotherm of aluminium oxide shows large hysteresis loop characterizing mesoporous nature of H1 type (Fig. 3a). Whilst, the doped  $\text{Al}_2\text{O}_3$  samples with different sizes gold clusters show sorption isotherm from type H3 (Figs. 3b and 4a) according to IUPAC classification of hysteresis loops [44]. This means the hysteresis loop of non-doped  $\text{Al}_2\text{O}_3$  changed from H1 into H3 type by doping with gold clusters.

The specific surface area and pore volume values illustrate a decrease in doped samples compared to pure  $\text{Al}_2\text{O}_3$  (Table 1). This could give a hint on the localization of Au nanoclusters deep inside the pores affecting the pore volumes that by its turn decrease the surface area values. In concordance, the doped catalysts show decrease in average pore diameter value in comparison to pure  $\text{Al}_2\text{O}_3$  catalyst, the average pore diameter of  $\text{Al}_2\text{O}_3$  and 1%  $\text{Au}_{25}(\text{SG})_{18}/\text{Al}_2\text{O}_3$  catalysts are 145.44 and 83.69 Å, respectively (Table 1). The pore size distribution of doped and non-doped catalysts was determined by the BJH method (Figs. 3c and 4b). The results showed that the pore size of  $\text{Al}_2\text{O}_3$  Puralox SCCa-190HPV was uniform in one domain maximizing at 184 Å; as a broad band, whereas the doped catalysts showed a one maximum peak at 24.7 Å (sharp), (Figs. 3c and 4b), which confirms the doped catalysts have micro pores and very small numbers from mesoporous. The  $V_{a-t}$  plots of  $\text{Al}_2\text{O}_3$  Puralox SCCa-190HPV and 1%  $\text{Au}_{25}(\text{SG})_{18}/\text{Al}_2\text{O}_3$  catalysts exhibited a upward and downward deviation (Fig. 3d), this clearly suggests the presence of mesoporous and microporous nature in these two catalysts, respectively [45,46]. Table 1 gives the textural data obtained through the analysis of  $\text{N}_2$  sorption data of the prepared catalysts. The values of  $S_{\text{BET}}$  and  $S_t$  for all investigated clusters are close to each other which justify the correct choice of

standard t-curves for pore analysis and indicate the absence of ultra-micropores in this adsorbents [46,47].

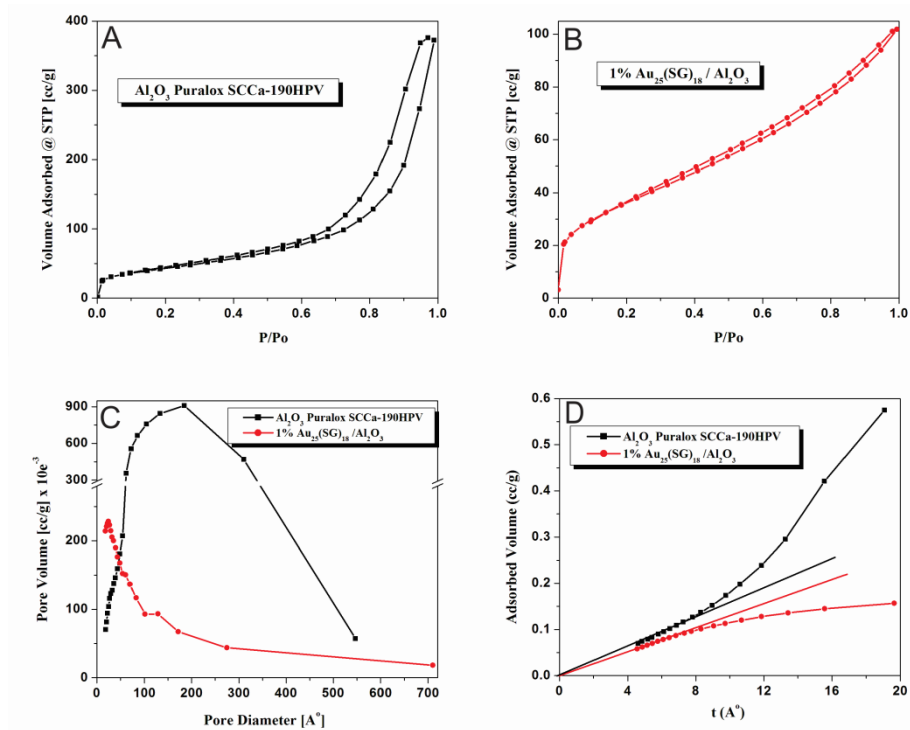


**Figure 3:** Nitrogen adsorption-desorption isotherms of Al<sub>2</sub>O<sub>3</sub> Puralox SCCa-190HPV (A) and 1% Au<sub>25</sub>(SG)<sub>18</sub>/Al<sub>2</sub>O<sub>3</sub> (B), the isotherms show mainly type H1 and H3 hysteresis loops according to IUPAC classification of hysteresis loops, respectively. The pore volume distribution curves of Al<sub>2</sub>O<sub>3</sub> Puralox SCCa-190HPV and 1% Au<sub>25</sub>(SG)<sub>18</sub>/Al<sub>2</sub>O<sub>3</sub> catalysts (C), the pore volume distribution curves show one broad peak at 184 Å, and one sharp peak at 24.7 Å, respectively. (D) The V<sub>a-t</sub> plots were exhibited a upward and downward deviation of Al<sub>2</sub>O<sub>3</sub> Puralox SCCa-190HPV and 1% Au<sub>25</sub>(SG)<sub>18</sub>/Al<sub>2</sub>O<sub>3</sub>, which confirms the presence of mesoporous and microporous nature in these two catalysts, respectively

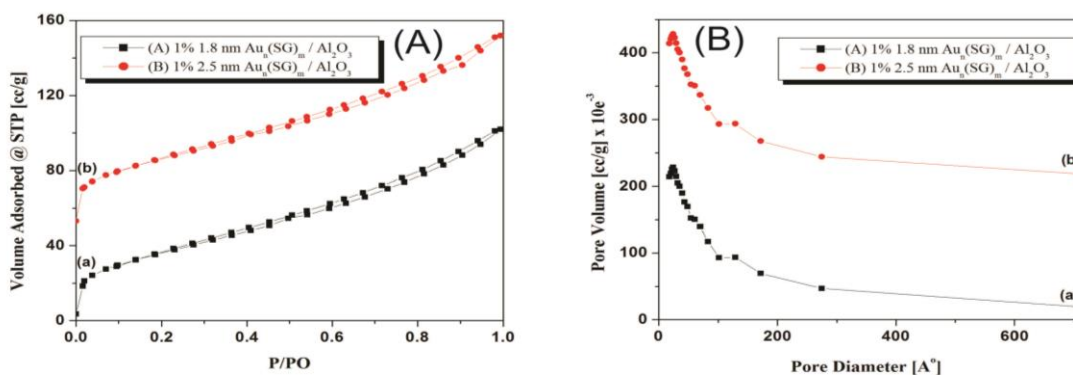


**Figure 4:** (A) Nitrogen adsorption-desorption isotherms of 1% Au<sub>n</sub>(SG)<sub>m</sub>/Al<sub>2</sub>O<sub>3</sub> (1.5 nm) and 1% Au<sub>n</sub>(SG)<sub>m</sub>/Al<sub>2</sub>O<sub>3</sub> (3 nm), the two isotherms show mainly type H3 hysteresis loops according to IUPAC classification of hysteresis loops. (B) The pore volume distribution curves of 1% Au<sub>n</sub>(SG)<sub>m</sub>/Al<sub>2</sub>O<sub>3</sub> (1.5 nm) and 1% Au<sub>n</sub>(SG)<sub>m</sub>/Al<sub>2</sub>O<sub>3</sub> (3 nm), the pore volume distribution curves show one sharp peak at 24.7 Å.

**Table 1:** Texture data obtained from the analysis of nitrogen sorption isotherms of prepared new catalysts.

No.	Catalysts	$S_{BET}$ ( $m^2g^{-1}$ )	$S_t$ ( $m^2g^{-1}$ )	Total pore volume ( $10^{-4}cc g^{-1}$ )	Average pore diameter ( $\text{\AA}$ )
1	$Al_2O_3$ Puralox SCCa-190HPV	154.69	151.22	5808.1	145.44
2	1% $Au_{25}(SG)_{18} / Al_2O_3$	135.26	135.85	2635.2	83.69
3	1% 1.5 nm $Au_n(SG)_m / Al_2O_3$	129.52	129.52	1561.8	48.23
4	1% 3 nm $Au_n(SG)_m / Al_2O_3$	122.08	121.71	1080.9	35.88

### 3.3. Catalytic Activity of prepared catalysts

In order to test the catalytic activity of the synthesised gold clusters catalysts, the well known catalytic reduction reaction of 4-NP with  $NaBH_4$  is used and the progress of the reaction is followed by UV-vis spectroscopy. The conversion of 4-NP to 4-AP versus stirring time was achieved for the three doped clusters on  $Al_2O_3$  as support (Fig. 5), whereas the non-doped  $Al_2O_3$  catalyst did not show any catalytic activity after 5 hours stirring under the same reaction condition.

Increasing the particles size of synthesized clusters from monodisperse clusters ( $Au_{25}$ ) compared to multidisperse clusters  $Au_n(SG)_m$  in average 1.5 nm and 3 nm reflect the effect of nanoparticles size on the catalytic activity. The size selected gold clusters on aluminium oxide (1%  $Au_{25}(SG)_{18}/Al_2O_3$ ) shows extreme catalytic activity in reduction of 4-NP into 4-AP (Fig. 5). 50 ml (2 mM) of 4-NP converted completely to 4-AP following 2 min stirring at room temperature in presence of 15 mg (0.3 g/L) 1%  $Au_{25}(SG)_{18}/Al_2O_3$  and 2.5 ml (2 M)  $NaBH_4$  as reducing agent (Fig. 5). The multidisperse gold clusters (1.5 and 3 nm) on  $Al_2O_3$  exhibited also high catalytic activity (Fig. 5). The 4-NP solution converted to 4-AP within 3 and 5 min stirring at the same reaction condition for 1.5 and 3 nm clusters, respectively (Fig. 5).

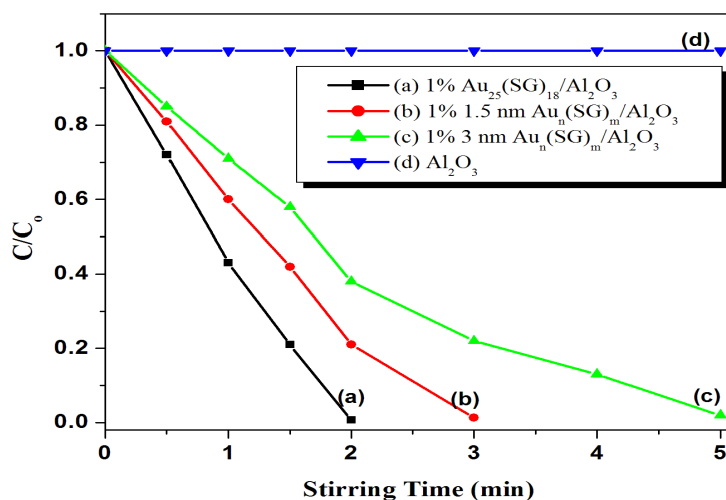


**Figure 5.** The change in the concentration of 4-NP with time during the reduction reaction by 1%  $Au_{25}(SG)_{18}/Al_2O_3$ , 1% 1.5 nm  $Au_n(SG)_m/Al_2O_3$ , 1% 3 nm  $Au_n(SG)_m/Al_2O_3$  and  $Al_2O_3$  Puralox SCCa-190HPV catalysts in the presence of aqueous  $NaBH_4$  (Reaction conditions: 50 ml [4-NP] = 2 mmol/L, 2.5 ml [ $NaBH_4$ ] = 2 mol/L, 15 mg catalyst, 1000 rpm).

The core/shell structure of  $Au_{25}(SR)_{18}$  superatoms consists of an  $Au_{13}$  icosahedral kernel and an exterior  $Au_{12}$  shell [7, 21]. Density functional theory (DFT) calculations [21,48–51] have shown distinct differences in charge distribution on the  $Au_{13}$  core and on  $Au_{12}$  shell. The  $Au_{13}$  core possesses 8 valence electrons ( $1s^21p^6$ ) [48,50]; these electrons originate from Au(6s) and are highly delocalized in the  $Au_{13}$  core, while the  $Au_{12}$  shell exhibits positive charges due to electron transfer from gold to sulfur atom in the thiolate ligands [50,51,52].

The suggested mechanism of 4-NP reduction over these protected gold clusters catalysts consist of two steps. The first one is diffusion and adsorption of 4-NP on the gold clusters surfaces, and then the electron transfer from the negatively charged  $BH_4^-$  to 4-NP via the AuNCs will proceed. The positively charged  $Au_{12}$  shell in  $Au_{25}(SG)_{18}$  clusters are demonstrated to be able to transfer the negative charge from  $NaBH_4$  to the 4-NP.

In this case, the electron transfer process depends upon the number of gold atoms present in the surface of clusters and the specific surface area of the clusters catalysts [53]. The reaction rate increases with an increase in the number of particles responsible for activating the reaction [54]. Thus, the slightly faster reaction of  $Au_{25}(SG)_{18}$  clusters than  $Au_n(SG)_m$  (1.5 and 3 nm) clusters can be attributed to two reasons, an increase in the number of surface Au atoms for the  $Au_{25}(SG)_{18}$  clusters,

and thus leads to an increased the electron transfer process from  $\text{NaBH}_4$  to the 4-NP, where the smaller metal particles possess higher redox potential, thus facilitating electrons transfer [55]. The second reason is the slightly increase on specific surface area of doped gold clusters on  $\text{Al}_2\text{O}_3$  from  $\sim 1$  nm to 3 nm (table 1).

$\text{Al}_2\text{O}_3$  had the largest pore diameter (14.5 nm), pore volume ( $0.58 \text{ cm}^3/\text{g}$ ) and specific surface area ( $154.69 \text{ m}^2\text{g}^{-1}$ ) values than the doped gold clusters (Table 1), however the non- doped aluminium oxide did not show any catalytic activity in 4-NP reduction (Fig. 5). Therefore this reaction depends on gold clusters not the pores properties and surface area of  $\text{Al}_2\text{O}_3$ .

We carried out control experiments in which 4-NP solution was stirred in the absence of any catalysts and in another time in absence of  $\text{NaBH}_4$  to exhibit no catalytic products were released. This result in good agreement with Mohamed et al. Results [56], they confirmed that the reduction of 4-NP to 4-AP using  $\text{NaBH}_4$  as the reducing agent is negligible if it is performed without catalyst [56].

To check the advantage of 1%  $\text{Au}_{25}(\text{SG})_{18}/\text{Al}_2\text{O}_3$ , 1% 1.5 nm  $\text{Au}_n(\text{SG})_m/\text{Al}_2\text{O}_3$  and 1% 3 nm  $\text{Au}_n(\text{SG})_m/\text{Al}_2\text{O}_3$  catalysts and its applicability to reuse [57-60], the reduction reaction of 4-NP was achieved with 0.3 g/L from each catalyst. Then the catalysts were collected at the end of the reaction and reused for a second cycle and the process repeated so on till four cycles keeping all other parameters constant (Fig. 6). The results revealed that catalyst shows a very good activity for four catalytic runs without loss in the 4-NP conversion. It can be conclude that the 1%  $\text{Au}_{25}(\text{SG})_{18}/\text{Al}_2\text{O}_3$ , 1% 1.5 nm  $\text{Au}_n(\text{SG})_m/\text{Al}_2\text{O}_3$  and 1% 3 nm  $\text{Au}_n(\text{SG})_m/\text{Al}_2\text{O}_3$  catalysts possesses high stability and it may be reusable for at least 4 runs, showing a good potential for practical applications (Fig. 6).

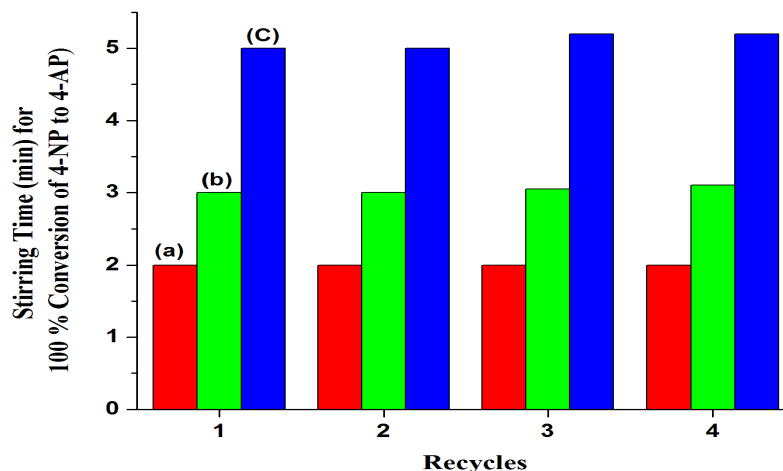


**Figure 6.** Repeated cycles up to 4 times illustrating the conversion yield of 4-NP after 2, 3 and 5 min stirring at room temperature over the (a) 1%  $\text{Au}_{25}(\text{SG})_{18}/\text{Al}_2\text{O}_3$ , (b) 1% 1.5 nm  $\text{Au}_n(\text{SG})_m/\text{Al}_2\text{O}_3$  and (c) 1% 3 nm  $\text{Au}_n(\text{SG})_m/\text{Al}_2\text{O}_3$  catalysts, respectively. The experimental conditions were kept constant.

## 4 Conclusions

In this work we have synthesized three different size gold clusters protected by L-glutathione.  $\text{Au}_{25}(\text{SG})_{18}$  and 1.5 nm and 3 nm  $\text{Au}_n(\text{SG})_m$  clusters are deposited over aluminium dioxide ( $\text{Al}_2\text{O}_3$  Puralox SCCa-190HPV). The obtained catalysts exhibited superior catalytic activity and stability during the heterogeneous catalytic reduction of 4-nitrophenol in presence of aqueous  $\text{NaBH}_4$  without using light. The results showed that the 1%  $\text{Au}_{25}(\text{SG})_{18}/\text{Al}_2\text{O}_3$  catalyst exhibited the best catalytic activity in the reduction of 4-NP into 4-aminophenol (4-AP) and revealed 100% conversion following 2 min stirring at room temperature. 1.5 nm and 3 nm gold clusters exhibited also a high conversion at similar reaction conditions, but the stirring time was increased little bit. The catalyst weight was used in this reaction 0.3 g/L. The reduction reaction of 4-NP was followed by UV-vis spectroscopy. Transmission electron microscopy was used to investigate the particles sizes of the prepared clusters. Specific surface area  $S_{\text{BET}}$ , pore volume and average pore diameter for prepared clusters over alumina were investigated using nitrogen adsorption-desorption at  $-196^\circ\text{C}$ . 1%  $\text{Au}_{25}(\text{SG})_{18}/\text{Al}_2\text{O}_3$  catalyst shows high stability and recyclability in 4-NP reduction reaction. The extreme catalytic activity of the small gold clusters  $\text{Au}_n(\text{SG})_m$  attribute to the partial positive charges on the surface Au atoms.

## Acknowledgements

This work is supported by Assiut University, Egypt.

## References

- [1] M. S. Chen, D. W. Goodman, *Science* 306 (2004) 252.
- [2] Y. Zhu, H. Qian, B. A. Drake, R. Jin, *Angew. Chem., Int. Ed.* 49 (2010) 1295.
- [3] H. Tsunoyama, N. Ichikuni, H. Sakurai, T. Tsukuda, *J. Am. Chem. Soc.* 131 (2009) 7086.
- [4] Y. Zhu, Z. Wu, C. Gayathri, H. Qian, R. R. Gil, R. Jin, *J. Catal.* 271 (2010) 155.
- [5] Y. Zhu, H. Qian, R. Jin, *Chem. Eur. J.* 16 (2010) 11455.
- [6] X. Nie, C. Zeng, X. Ma, H. Qian, Q. Ge, H. Xua, R. Jin, *Nanoscale* 5 (2013) 5912.
- [7] B. Y. Zhu, H. Qian, M. Zhu, R. Jin, *Adv. Mater.* 22 (2010) 1915-1920.
- [8] W. C. Ketchie, Y. L. Fang, M. S. Wong, M. Murayama, R. J. Davis, *J. Catal.* 250 (2007) 94.
- [9] H. H. Kung, M. C. Kung, C. K. Costello, *J. Catal.* 216 (2003) 425.
- [10] M. M. Schubert, S. Hackenberg, A. C. van Veen, M. Muhler, V. Plzak, R. J. Behm, *J. Catal.* 197 (2001) 113.
- [11] M. Haruta, N. Yamada, T. Kobayashi, S. Iijima, *J. Catal.* 115 (1989) 301.
- [12] L. Wen, J. K. Fu, P. Y. Gu, B. X. Yao, Z. H. Lin, J. Z. Zhou, *Appl. Catal., B* 79 (2008) 402.
- [13] Y. J. Chen, C. T. Yeh, *J. Catal.* 200 (2001) 59.
- [14] X. Huang, X. Zhou, S. Wu, Y. Wei, X. Qi, J. Zhang, F. Boey, H. Zhang, *Small* 6 (2010) 513.
- [15] M. Farrag, M. Tschurl, U. Heiz, *Chem. Mater.* 25 (2013) 862.
- [16] M. Farrag, M. Tschurl, A. Dass, U. Heiz, *Phys. Chem. Chem. Phys.* 15 (2013) 12539.
- [17] M. Zhu, E. Lanni, N. Garg, M. E. Bier, R. Jin, *J. Am. Chem. Soc.* 130 (2008) 1138.
- [18] H. Qian, Y. Zhu, R. Jin, *ACS Nano* 2009, 3, 3795.
- [19] Y. Negishi, M. Mizuno, M. Hirayama, M. Omatoi, T. Takayama, A. Iwase, A. Kudo, *Nanoscale* 5 (2013) 7188–7192.
- [20] M. R. Branham, A. D. Douglas, A. J. Mills, J. B. Tracy, P. S. White, R. W. Murray, *Langmuir* 22 (2006) 11376.
- [21] M. Zhu, C. M. Aikens, F. J. Hollander, G. C. Schatz, R. Jin, *J. Am. Chem. Soc.* 2008, 130, 5883.
- [22] E. S. Shibu, M. A. Habeeb Muhammed, T. Tsukuda, T. Pradeep *J. Phys. Chem. C*, 112 (2008) 12168.
- [23] M. Farrag, M. Thämer, M. Tschurl, T. Bürgi, U. Heiz, *J. Phys. Chem. C* 116 (2012) 8034.
- [24] C. V. Rode, M. J. Vaidya, R. V. Chaudhari, *Org. Process Res. Dev.* 3 (1999) 465–470.
- [25] K.R. Westerterp, E.J. Molga, K.B. van Gelder, *Chem. Eng. Process.* 36 (1997) 17–24.
- [26] H.W. Shih, M. N. Vander Wal, R.L. Grange, D. W. C. Mac Millan, *J. Am. Chem. Soc.* 132 (2010) 13600–13603.
- [27] H. Lu, H. Yin, Y. Liu, T. Jiang, L. Yu, *Catal. Commun.* 10 (2008) 313–318.
- [28] Y. Mei, Y. Lu, F. Polzer, M. Ballauff, *Chem. Mater.* 19 (2007) 1062.
- [29] Y. Wang, G. Wei, F. Wen, X. Zhang, W. Zhang, L. Shi, *J. Mol. Catal. A: Chem.* 280 (2008) 1.
- [30] Y. Lu, Y. Mei, R. Walker, M. Ballauff, M. Drechsler, *Polymer* 47 (2006) 4985.
- [31] L. Liu, B. Qiao, Y. Ma, J. Zhang, Y. Deng, *Dalton Trans.* 19 (2008) 2542.
- [32] J. Ning, J. Xu, J. Liu, H. Miao, H. Ma, C. Chen, X. Li, L. Zhou, W. Yu, *Catal. Commun.* 8 (2007) 1763.
- [33] G. Zhang, L. Wang, K. Shen, D. Zhao, H.S. Freeman, *Chem. Eng. J* 141 (2008) 368.
- [34] A. Corma, P. Serna, *Science* 313 (2006) 332.
- [35] N.S. Chaubal, M.R. Sawant, *J. Mol. Catal. A: Chem.* 261 (2007) 232.
- [36] Y. Mei, Y. Lu, F. Polzer, M. Ballauff, *Chem. Mater.* 19 (2007) 1062.
- [37] Y. Wang, G. Wei, F. Wen, X. Zhang, W. Zhang, L. Shi, *J. Mol. Catal. A: Chem.* 280 (2008) 1.
- [38] L. Liu, B. Qiao, Y. Ma, J. Zhang, Y. Deng, *Dalton Trans.* 19 (2008) 2542.
- [39] J. Liu, G. Qin, P. Raveendran, Y. Ikushima, *Chem. Eur. J.* 12 (2006) 2131–2138.
- [40] M.M. Mohamed, M.S. Al-Sharif, *Applied Catalysis B: Environmental* 142–143 (2013) 432–441
- [41] Z. Wu, J. Chen, R. Jin *Adv. Funct. Mater.* 21 (2011) 177–183.
- [42] Z. Wu, J. Suhan, R. Jin, *J. Mater. Chem.* 19 (2009) 622.
- [43] M. M. Alvarez, J. T. Khoury, T. G. Schaaff, M. N. Shafiqullin, I. Vezmar, R. L. Whetten, *J. Phys. Chem. B* 101 (1997) 3706.
- [44] IUPAC Recommendations *Pure Appl. Chem.* 66 (1994) 1739.
- [45] G. Leofanti, M. Padovan, G. Tozzola, B. Venturelli, *Catalysis Today* 41 (1998) 207–219.
- [46] M. Th. Makhlof, B. M. Abu-Zied, T.H. Mansoure, *Applied Surface Science* 274 (2013) 45–52.
- [47] W. M. Shaheen, A. A. Zahrn, G.A. El-Shobaky, *Colloids and Surfaces A: Physicochemical and Engineering Aspects*, 231 (2003) 51–65.
- [48] J. Akola, M. Walter, R. L. Whetten, H. Häkkinen, H. Gronbeck, *J. Am. Chem. Soc.* 130 (2008) 3756.
- [49] M. Walter, J. Akola, O. Lopez-Acevedo, P. D. Jadzinsky, G. Calero, C. J. Ackerson, R. L. Whetten, H. Grönbeck, H. Häkkinen, *Proc. Nat. Acad. Sci. USA* 105 (2008) 9157.
- [50] M. Zhu, C. M. Aikens, M. P. Hendrich, R. Gupta, H. Qian, G. C. Schatz, R. Jin, *J. Am. Chem. Soc.* 131 (2009) 2490.
- [51] C. M. Aikens, *J. Phys. Chem. C* 112 (2008) 19797.

- [52] Z. Wu, R. Jin, ACS Nano 3 (2009) 2036.
- [53] K. Kuroda, T. Ishida, M. Haruta, J. Mol. Catal. A 298 (2009) 7.
- [54] S. Kundu, S. Lau, H. Liang, J. Phys. Chem. C 113 (2009) 5150–5156.
- [55] J. Liu, G. Qin, P. Raveendran, Y. Ikushima, Chem. Eur. J. 12 (2006) 2131–2138.
- [56] M. M. Mohamed, M.S. Al-Sharif, Mater. Chem. Phys. 136 (2012) 528–537.
- [57] M. Farrag, J. Mol. Catal. A: Chem. 413 (2016) 67.
- [58] M. Farrag, J. Photochem. Photobiol. A: Chem. 318 (2016) 42.
- [59] M. Farrag, Micropor. Mesopor. Mat., 232, 248-255 (2016).
- [60] M. Farrag, Mater. Chem. Phys., 180, 349-356 (2016).